

Pulse Shapes Techniques Application to Intense Pulsed Light for skin lesions

Jeun-Jong Baeg¹, Han-Ho Tac², Whi-Young Kim*

¹(Department of Electronic engineering, Gyeongnam National University of Science and Technology, Korea

²(Department of Electronic engineering, Gyeongnam National University of Science and Technology, Korea

*(Department of Biomedical Engineering Dongju college University, Korea)

Abstract: Intense pulsed light causes changes in the blood vessels inside the corium after passing through the skin. In addition, it affects fibroblasts, imparts elasticity to skin collagen and induces filling of the skin epidermis. According to several diagnostic purposes, a method for controlling the operating time due to the output pulse can be applied by changing the control pulse. Various output pulses are needed for different treatment methods of Intense Pulsed Light(IPL) in accordance with the skin color and lesion. Since the heating pulse intensity, pulse width and pulse shape need to be tailored to the skin condition, there is some restriction in terms of the range of treatments as well as the diagnosis with the existing pulse techniques. A population inversion was induced by heat pumping a Xe Lamp through a $V_{variable}$ Pulse Beam Shapes. The necessary discharge energy was charged through the network to produce various current pulses. By grafting a one chip Microprocessor and $V_{variable}$ Pulse Beam Shapes of an AVR affiliation, a circuit was designated from the 1st to 8th levels. Xenon gas was used as the medium. The output, pulse width and pulse count was $15J/cm^2 \sim 45J/cm^2$, $0.5ms \sim 15ms$, and $1 Hz \sim 3 Hz$, respectively. As a result, the corresponding current waveform could be recognized through a PSPICE simulation and the experimentally determined waveform. Moreover, both the efficiency and maximum output changed according to the results of the Discharging Light of $V_{variable}$ Pulse Beam Shapes.

Keywords: Intense Pulsed Light, Xe Lamp, Pulse Beam Shapes, PSPICE, AT80S8535

I. Introduction

Dr. Vitor invented a new treatment method called photo rejuvenation, which employs a discharging light of multiple wavelengths not a singular wavelength. Lasers are available for partial treatment but only one wavelength is used [1-3]. On the other hand, intense pulsed light (IPL) has an extensive treatment range. A 500nm wavelength is suitable for treating blood vessel disease, whereas a 700nm wavelength is effective for pigment disease. However, IPL used a range of wavelengths, 515~ 1,200nm. Wavelength filters can remove the light below a certain light waveform length[4-5]. A 500nm filter removes the entire wavelength below 590nm. The IPL variables include the skin type, energy, waveform length and examination period.

The treatment is operated by adjusting 4 variables according to the lesion. Generally, the treatment effect is likely to improve with increasing energy [6-9]. However, a much shorter wavelength can cause significant damage to the skin and have less penetrability. The energy should be sufficient and the wavelength (515-1200nm), pulse width and time, as well as the delay time between pulses should be adjusted accordingly [10]. Theoretically, it would be the best to use the energy appropriate for the skin type. Nevertheless, a different reaction from that anticipated can occur during treatment. In particular, light with a low wavelength is more effective due to hot flushes and vasodilatation.

To cure a stretched blood vessel, the energy should be increased by adjusting with light of a high wavelength because it needs to penetrate deep inside[10]. Adjustments of the light exposure time are needed because the skin can be damaged as the energy is increased. Because there is the possibility of scab formation caused by the absorption of energy by the pigment of dark skin, the energy normally decreases, light with a higher wavelength tends to be exposed, and the adjustment operates to expose light for a long period.

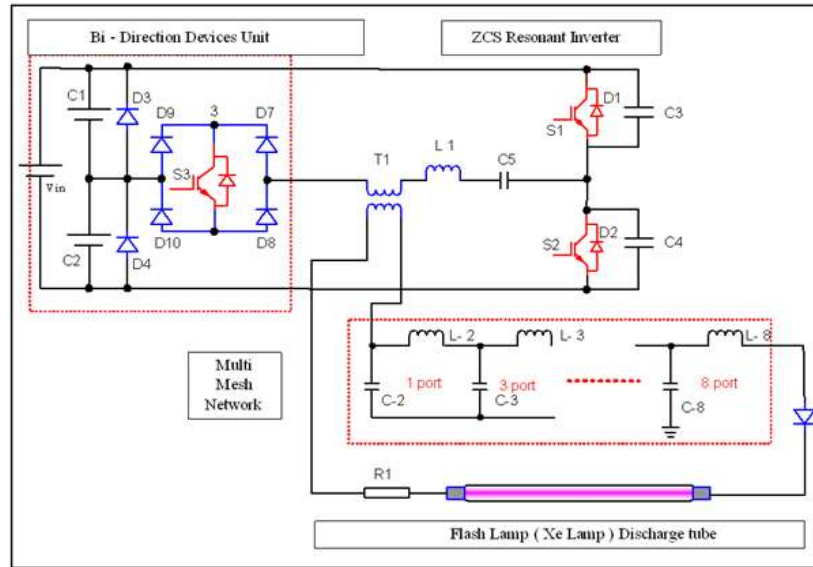


Fig. 1 Diagram of the proposed Intense Pulsed Light system

Therefore, those people with a dark skin color are less likely to have effective treatment than people with lighter skin. In this study, a population inversion was induced by light pumping with a Xe Lamp through a Mesh Network[7]. Only the discharge energy was recharged and a range of current pulses that the load demands were obtained. A PSPICE simulation and experiment waveform characteristic were compared with the Xe Lamp output current waveform, and an AT80S8535 one chip Micro Processor of AVR affiliation was used to drive, control and monitor the screen. The circuit was composed of a L-C composition from the 1st to 8th levels in a Discharging Light of $V_{variable}$ Pulse Beam Shapes. to acquire a range of pulse waveforms. Therefore, several output characteristics were organized according to the lesions in the body.

II. Materials And Methods

2-1. Composition

Figure 1 shows the proposed system, which can be divided into 4 areas. Firstly, the system is driven with one half of a direct current power supply using a bidirectional device. The rated current was not increased while driving, but the voltage and current control were composed of a dead-beat controller to maintain a stable output voltage regardless of the load variations. Secondly, the pulse repetition rate and pulse width were utilized by controlling the current density, which employs a resonance converter by checking for zero using an AVR one-chip. Thirdly, various treatment pulses can be produced by the Discharging Light of Multiple Wavelengths, which performs a significant function. Lastly, the discharge tube of a flash lamp is used.

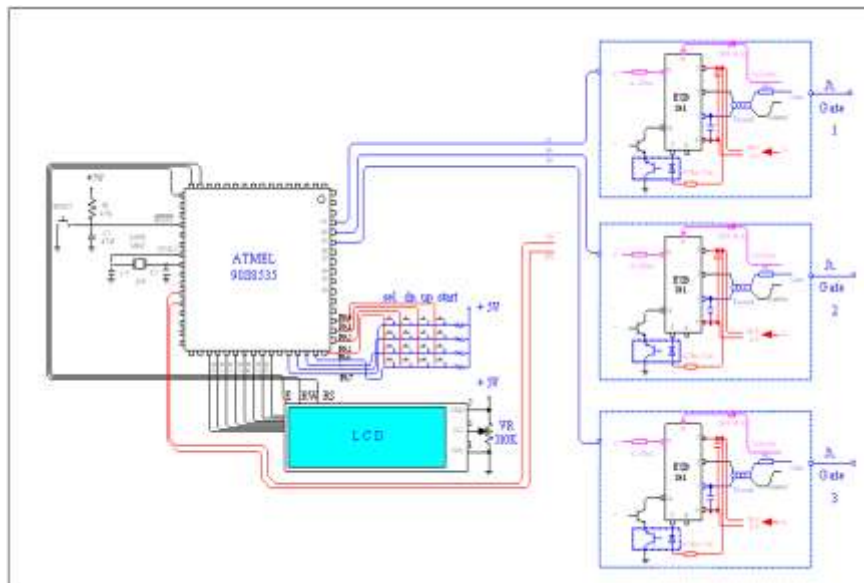


Fig. 2 AVR-one-chip control and drive circuit

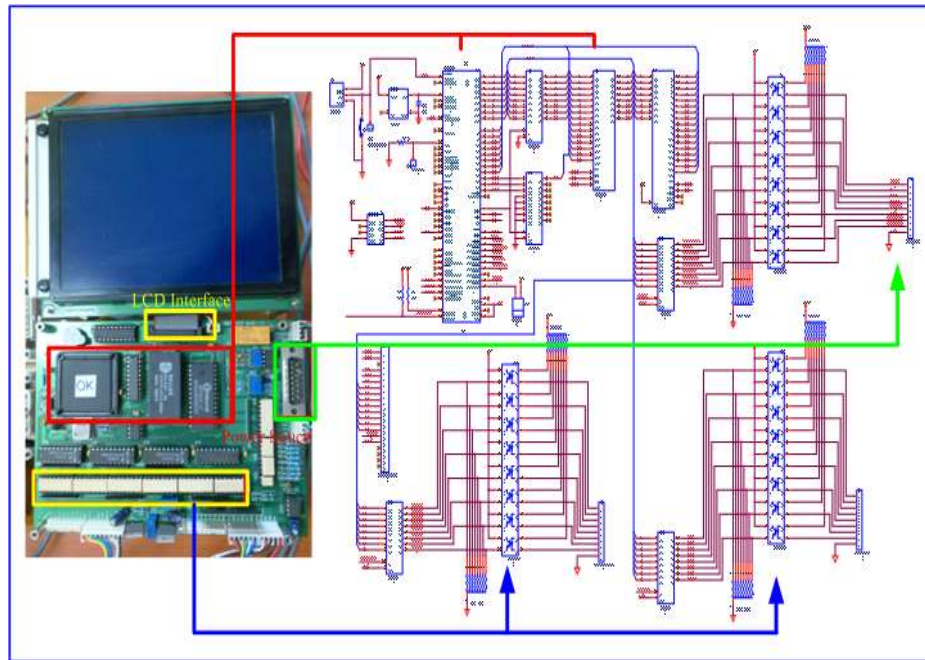


Fig. 3 Shows a circuit for the display and control PCB board.

2-2. Installation

The power supply is largely formed by a bidirectional device (compensating circuit of a generating current) and a half bridge (ZCS resonance converter). A smooth condenser with a parallel frequency and a large output capacitor were adapted because an excessive peak current is produced by the main circuit of the ZCS direct current resonance converter of a compensated generating current. The ZCS series resonance converter consisted of a switching device (S1, S2), resonance inductor (L1) and capacitor (c1, c2), and a generating current device (S3).

The current flowed through the switching device and a capacitor performed the on/off function. Hence, there is no switching loss and high repetition movement as fundamentals. Figure 1 presents the composition of the basic circuit to stabilize the unstable lamp operation after operating an inductor (L2 100uH) between the IGBT drive and protection circuit, and the magnetic switch to the simmer of the additional Xenon Lamp.

Figure 1 shows that the existing method drives the simmer using the high voltage with the chalk method using the Xenon Lamp to Full Bridge of the indirect method. Although the simmer has a noise inside system with a large number of problems during NG, the experiment can be miniaturized with a stable simmer and high insulation effect by adapting a pulse transformer and triplication insulation wire method into the simmer circuit.

2-3. Pulse Shapes

A flash lamp can form a population inversion of a medium with light pumping and construct a MW that consists of a resistance (R), capacitance (C) and inductance (L) to supply energy towards the pumping light source. The flash lamp is operated as a single or MW. The network recharges the discharging energy to have demanded current pulse when being sent to the flash lamp.

If the discharge is insufficient, an inverse current flows into the flash lamp, which shortens the lifespan of the flash. In addition, the discharging efficiency decreases, which results in critical damping of the current pulse flowing into the flash lamp. The condition of critical damping is indicated in equation (1) and (2). The voltage-current characteristics of such a high current flash are the same as follows:

$$V = \pm K_0 \sqrt{|i|} \quad (1)$$

$$K_0 = \frac{Kl}{d[\Omega - \sqrt{A}]} \quad (2)$$

where l, d, and K indicate the variable related to the length of flash lamp, diameter and type of gas, and pressure, respectively. A nonlinear differential equation of the circuit can be expressed as follows:

$$\frac{dl}{dr} + [\alpha + \beta \sqrt{|l|}] \sqrt{|l|} + \int_0^r l dr = 1 \quad (3)$$

$$I = i \sqrt{\frac{LC}{V_0}} \quad (4)$$

$$r = \frac{t}{\sqrt{LC}} \quad (5)$$

$$\alpha = \frac{k}{\sqrt{V_0 Z_0}} \quad (6)$$

$$\beta = r \sqrt{LC} \quad (7)$$

$$Z_0 = \sqrt{LC} \quad (8)$$

Where R is the total resistance of circuit except self-resistance of flash lamp and α is the damping parameter, which indicates the discharging characteristic of the flash lamp. When the resistance of a circuit is very low, the discharging characteristic of the flash lamp is determined by the capacitance C, entry voltage V_0 and inductance L in the case of proper MW ($\beta \approx 0$). The equation can be expressed as follows:

$$C^3 = 0.09 \frac{E_0 t_p^2}{K_0^4} \quad (9)$$

$$L = \frac{t_p^2}{9C} \quad (10)$$

$$E_0 = \frac{1}{2} C V_0^2 \quad (11)$$

$$Z_0 = \sqrt{LC} \quad (12)$$

$$\alpha = \frac{k}{\sqrt{V_0 Z_0}} \quad (13)$$

The demanded pulse form can be obtained by determining L and C using equation (13) from equation (9). These pulse forms have a significant relationship with the discharge of the flash lamp, and whether the discharging current of the flash lamp performs critical damping with time can be confirmed when the damping parameter is $\alpha = 0.75$.

At this point, critical damping means considerable discharge over a short period. An approximate equation of the multiple circuits determined by the particular impedance of the electric network in a V_{variable} Pulse Beam Shapes circuit is indicated.

$$Z_n = \sqrt{\frac{L_T}{C_T}} \quad (14)$$

$$t_p = 2 \sqrt{\frac{L_T}{C_T}} \quad (15)$$

$$C_p = \frac{t_p}{2Z_n} \quad (16)$$

$$L_p = \frac{t_p Z_n}{2} \quad (17)$$

$$V = \sqrt{\frac{2E}{C_T}} \quad (18)$$

$$i_p = \frac{V_0}{2Z_n} \quad (19)$$

Where, Z_n : Particular impedance of the electric network [Ω]

L_T : Total inductance of the mesh network [μH]

C_T : Total capacitance of the mesh network [μF]

t_p : Current pulse width [s]

V_0 : Recharging voltage [V]

E: Flash lamp entry energy [J]

i_p : Maximum current flowing over the flash lamp [A]

As shown in Figure 1, the 1st column mesh set, C_T , of the main circuit is $480 \mu F$, $L_T = 240 \mu H$. Therefore, the capacitance of the 2nd column mesh circuit, which can recharge the same entry energy, C_1 and C_2 , becomes $240 \mu F$, and the inductance L_1 and L_2 becomes $120 \mu H$. The 3rd mesh capacitance, C_1 , C_2 and C_3 , are $160 \mu F$, and the inductance L_1 , L_2 and L_3 become $80 \mu H$. C and L of the 6th and 8th mesh are also determined automatically by each singular. The C and L value of each singular is determined automatically using the same method based on an increasing number of meshes when $C_T = 960 \mu F$, $C_T = 240 \mu F$, when $L_T = 480 \mu H$ and $L_T = 120 \mu H$.

2-4. Control Unit

Figure 2 shows the role of the IGBT drive that is formed using the AVR one-chip Micro Processor and time control circuit. Fig 2, AVR-one-chip control and drive circuit. Fig 3, Shows a circuit for the display and control PCB board. Fig 4, measure waveform of the ZCS Inverter (1: Timing signal AVR 2, 2: S1, S2 control signal AVR 1, 3: S4 control signal AVR 1, 4: S3 control signal AVR 1).

The drive is formed into 4 sections by the control circuit. The first is composed of a keyboard to enter the time control, and the second is a LCD indication unit that indicates the entered control state.

The third section is the AVR Microsoft Processor of ATMEL, which is a core of the control circuit that provides many interfaces. The fourth section performs amplification to turn on the IGBT and MW as the drive support. The operation of the control circuit is the same as follows. If the information of the delay time is entered through a keyboard, it is delivered to the AVR, which prints out each different signal caused by the arranged program.

The series of the signals printed out from the AVR is the LCD display signal and the signal to drive the IGBT with each demanded delay time in the switching circuit. The IGBT drive signals operate the related signals with accurate confirmation as the time entered through the key board after driving S1, S2 and S3.

Figure shows the inverter output current waveform and control signal, and Figure shows all types of experimental timing signals. Fig measured waveform of the ZCS Inverter (1: Inverter output current, 2: Recharging current, 3: S1, S2 signal waveform, 4: S4 control signal). Figure 4 Measured Waveform of the ZCS Inverter (1: Timing signal AVR 2, 2: S1, S2 control signal AVR 1, 3: S4 control signal AVR 1, 4: S3 control signal AVR 1).

Fig 1, 3 Schematic figure of intense pulse light with variable pulse beam shapes. Fig. 7 Experimental apparatus(includes Optics and capacitor charger). When the total capacitance $CT(480\mu F)$ and total inductance $LT(240\mu H)$ are on the 6th level(a) Flash Lamp current simulation waveform (b) Flash Lamp current waveform and the output beam. The observed flash lamp and current waveform as well as the mesh and beam profile when $CT = 480 \mu F$ and $LT = 240 \mu H$.

The profile of the IPL output beam was measured using a pin-type photo diode (model name: An-tel ARS-1). When the mesh number was 6, the current pulse width t_p was approximately $680\mu s$. Figure (b) shows the current waveform and Figure (a) presents the profile of the output beam. Q_{TH} is the discharging quantity of the electric charge consumed for the reversal distribution formation and Q_L is the discharging quantity of the electric charge contributing to the actual IPL output. Significant IPL output occurs when Q_L makes a larger contribution to the IPL output than the actual current waveform.

Fig 5, Power module of intense pulse light with variable pulse beam shapes. Fig 6, Experimental apparatus(includes Optics and capacitor charger). Fig 8, When the total capacitance $CT(480\mu F)$ and total inductance $LT(240\mu H)$ are on the 6th level (a) Flash Lamp current simulation waveform (b) Flash Lamp current waveform and the output beam. Fig 8, When the total capacitance $CT(480\mu F)$ and total inductance $LT(240\mu H)$ are on the 8th level (a) Flash Lamp current simulation waveform (b) Flash Lamp current waveform and experimental waveform of the output beam.

III. Experiment Results

The results of the PSpice simulation waveform, which appears to be similar to the current waveform of the actual flash lamp. The IPL output was measured using an energy meter (model name: Scientech D300C), as the entry energy increased with increasing authorized voltage. When the entry energy is 40J, the mesh at the 1st, 6th, and 8th levels has an IPL output of 44mJ, 2808mJ, and 2392mJ, respectively.

Therefore, the optimum mesh is at the 6th level. The discharging quantity of the electric charge consumed immediately before oscillation was determined to be 52.3 by obtaining the area where Q_{TH} and Q_L take over the current waveform of the LeCroy 9304A. The bottom part of when the number of meshes is the 8th level and the discharging quantity of the electric charge consumed immediately before oscillation is 65.8. Therefore, the mesh at the 6th level contains a lower Q_{TH} of consumed discharging quantity of electric charge immediately before oscillation than the mesh at the 8th level. On the other hand, Q_L , which contributes to the

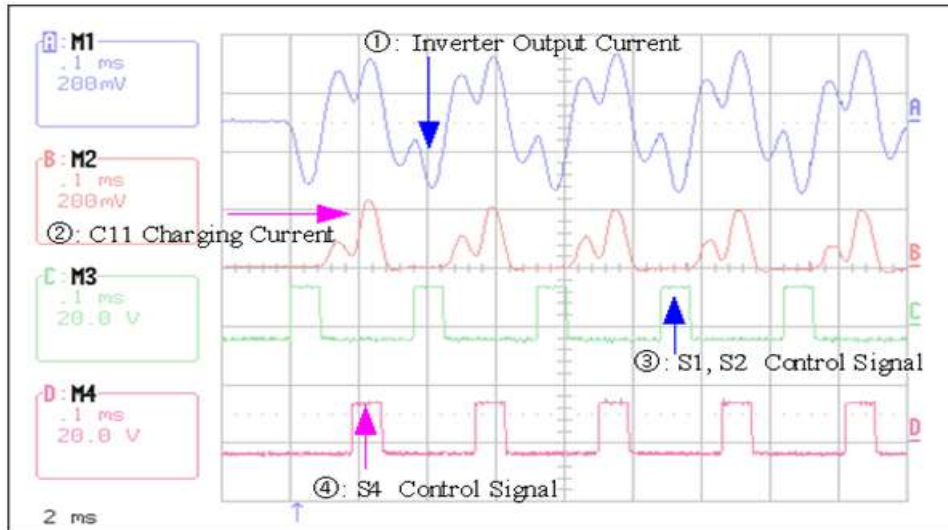


Fig.6 Measured waveform of the ZCS Inverter (1: Timing signal AVR 2, 2: S1, S2 control signal AVR 1, 3: S4 control signal AVR 1, 4: S3 control signal AVR 1)

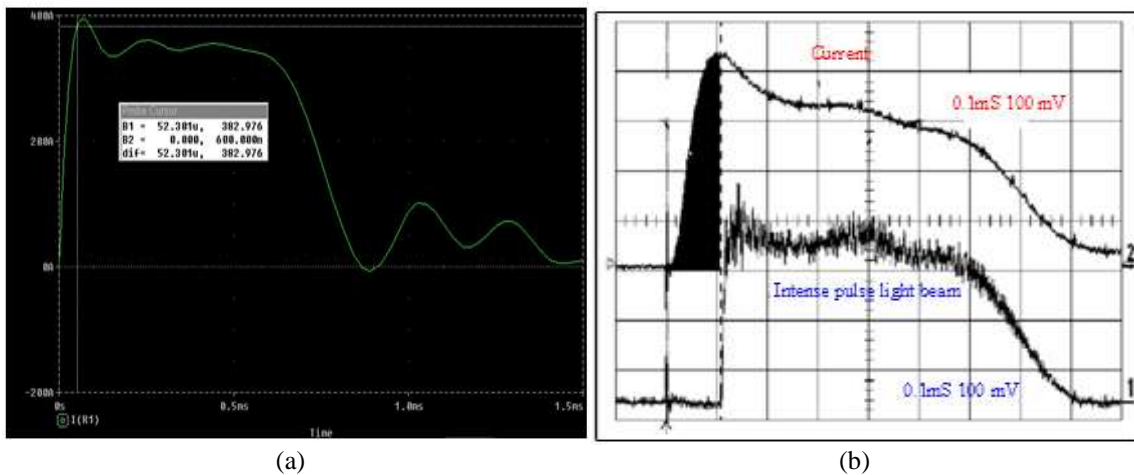


Fig. 7 When the total capacitance $C_T(480\mu F)$ and total inductance $L_T(240\mu H)$ are on the 6th level (a) Flash Lamp current simulation waveform (b) Flash Lamp current waveform and the output beam

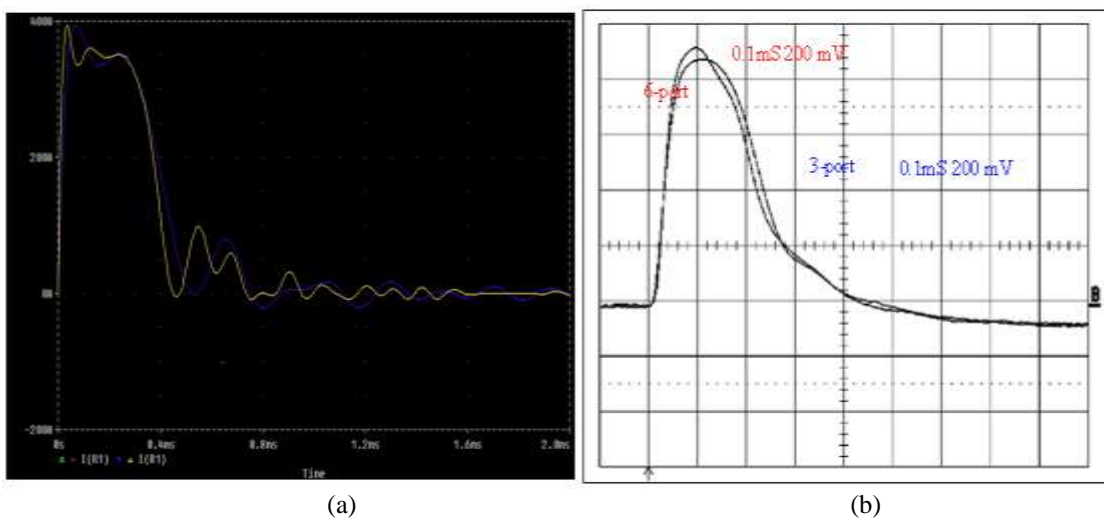


Fig. 8 When the total capacitance $C_T(480\mu F)$ and total inductance $L_T(240\mu H)$ are on the 8th level (a) Flash Lamp current simulation waveform (b) Flash Lamp current waveform and experimental waveform of the output beam

Therefore, the mesh at the 6th level occupies a comparatively larger area for QL than the mesh at the 3rd or 8th levels. Therefore, an increasing IPL output can be recognized. Figure shows the IPL output in accordance with the mesh after setting CT = 960 and LT = 480. In the case of authorizing an entered energy of 40J, the mesh at the 3rd, 6th and 8th levels has an IPL output of 504mJ, 1,112mJ and 836mJ, respectively.

Therefore, the ideal mesh is at the 6th level. Fig 8, When the total capacitance CT(480uF) and total inductance LT(240uH) are on the 8th level (a) Flash Lamp current simulation waveform (b) Flash Lamp current waveform and experimental waveform of the output beam. Fig. 9 (a) the black, yellow, white, Pigment for the clinical treatment algorithm. (b) the black, yellow, white, vascular clinical treatment algorithm for (c) the black, yellow, white, clinical treatment algorithm for the rejuvenation (d) the black, yellow, white, hair removal for the clinical treatment algorithm shows. Fig, Total capacitance CT [960 μF] and total inductance LT [480μH] output energy vs. the number of intense pulse light with variable pulse beam shapes

V. Conclusion

The existing oval type as well as the performance and efficiency were compared through the preparation and production of an IPL. This study examined the cross-check current waveform IPL beam profile and IPL output at mesh levels between the 1st and 8th levels, which is identical to the total capacitance of the main power supply and total inductance.

The operating experiment by planning and producing a bidirectional device, resonance converter and V_{variable} Pulse Beam Shapes, revealed a maximum efficiency of approximately 8.1%, which is more likely to be compact compared to the existing type. Moreover, planning and producing is simple. A comparison of the authorized output characteristics of the circuit at the 1st to 8th levels, where the same power is entered when the current pulse width is < 500 μs, revealed a maximum output of 2,712mJ from the mesh at the 3rd level, which conforms to the PSPICE simulation.

A comparison of the authorized output characteristic of the circuit at the 1st to 8th levels, where the same power was entered when the current pulse width is > 500 μs, revealed a maximum output of 2808mJ from the mesh at the 6th level, which conforms to the PSPICE simulation.

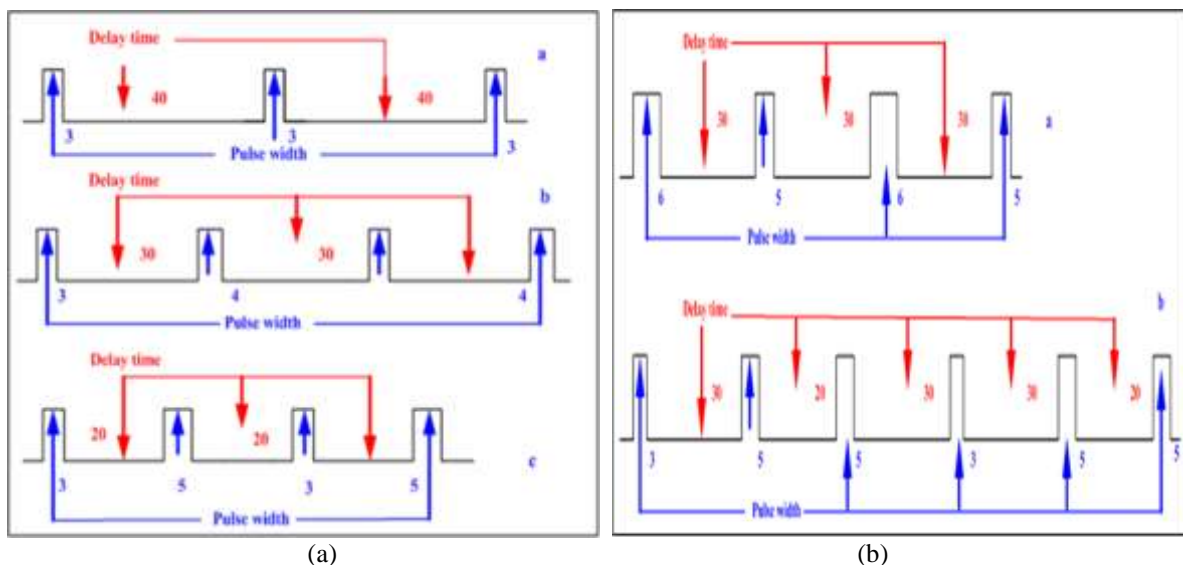


Fig. 9 (a) the black, yellow, white, Pigment for the clinical treatment algorithm. (b) the black, yellow, white, vascular clinical treatment algorithm for the black, yellow, white, clinical treatment algorithm for the rejuvenation the black, yellow, white, hair removal for the clinical treatment algorithm shows.

Acknowledgements

This work was supported by Piece College (U.S.A.) Grant 2017.

References

- [1]. Hyun-mo Koo, Changes in Poly ADP ribose polymerase immune response cells of Cerebral Ischaemia Induced rat by Transcranial Magnetic Stimulation of Alternating Current approach. J of Magnetics., 2014, 19(4) pp. 357-364.
- [2]. Wassermann E, Oxford Handbook of Transcranial Magnetic Stimulation, Oxford University Press, Oxford, 2007.
- [3]. Frackowiak RSJ, Friston KJ, Frith C et al., Human Brain Function, 2nd edn., Academic Press, San Diego, 2003.
- [4]. Devinsky O, Beric A, Electrical and Magnetic Stimulation of the Brain and Spinal Cord, Raven Press, 1993.

- [5]. George MS, Transcranial Magnetic Stimulation in Clinical Psychiatry, American psychiatric publishing, inc, 2006.
- [6]. Whi-Young Kim, The Characteristics on the change of Cerebral cortex using Alternating Current Power application for Transcranial Magnetic Stimulation. J of Magnetics., 2014, 19(2) pp. 197-204.
- [7]. Levy WJ, Magnetic Motor Stimulation Basic Principles and Clinical Experience, Elsevier, 1991.
- [8]. Ha DH, 3 Stage 2 switch application for transcranial magnetic stimulation, J Magnet 16(3):234–239, 2011.
- [9]. Wallisch P, MATLAB for Neuroscientists, Academic Press, 2010.
- [10]. Friston KJ, Statical Parametric Mapping, Academic Press, 2006.
- [11]. Sun-Seob Choi, “Treatment pulse application for Magnetic Stimulation ”, journal of Biomedicine and Biotechnology, 2011, article ID 278062, 6page,doi: 10.1153/2011/278062.